Quest Journals
Journal of Research in Environmental and Earth Sciences
Volume 10 ~ Issue 11 (2024) pp: 22-34
ISSN(Online) :2348-2532
www.questjournals.org

Research Paper

Glacial-Interglacial Cycles over the Past 150,000 years of South-Eastern Arabian Sea from $\delta^{18}O$ Record

Bhadra Kumary SR[1]*, Gopakumar B[1], Manjunatha BR[2], Anil Kumar A[3], Shaniba V[4], Subhradeep Das[3]

[1](Geological Survey of India, Western Region, Jaipur, India)
[2](Department of Marine Geology, Mangalore University, Mangalore, India),
(Department of Civil Engineering, Dayananda Sagar College of Engineering, Bangalore, India)
[3] (Geological Survey of India, CHQ, 27, Jawaharlal Nehru Road, Kolkata, India)
[4](Geological Survey of India, M &CSD, OPEC-II, Vishakhapatanam, India)
*Corresponding author. E-mail: gopanbhadra@gmail.com

ABSTRACT: *This study aims to reconstruct the surface water productivity and related monsoonal intensity along the southwestern continental margin of India, over the last 150,000 years by utilizing the temporal variations of $\delta^{18}O$ and $\delta^{13}C$ isotopes in the planktic foraminifers (Globigerinoides ruber) from a sediment core obtained from the continental slope off Kochi, south-eastern India. The chronostratigraphy of the core is established on the basis of high resolution stable isotope record of planktic foraminifera (Globigerinoides ruber) and a few AMS radiocarbon ages. Down-core records of $\delta^{18}O$ and $\delta^{13}C$ show millennial scale variations of primary productivity and monsoonal intensity during past 150 kyr. Boundaries of the Marine isotope stages (MISs) were delineated in the core based on the visual comparison of the $\delta^{18}O$ with Martinson's (D. M. Martinson, N.G. Pisias, J.D. Hays, J. Imbrie, T.C. Moor Jr, N.J. Shackleton, Age dating and the orbital theory of the ice ages: development of a high resolution 0 to 300000 year chronostratigraphy, Quaternary Research, 1987* ***27****, p 1-29) and the SPECMAP data. From these studies it is inferred that the bottom of the core is about 150 kyrs, demarcating the paleoclimatic/paleoceanographic information covering MIS 1 to 6. Boundaries among MIS 6 and MIS 5, MIS 5 and MIS 4, MIS 4 and MIS 3, MIS 3 and MIS 2 and MIS 2 to MIS 1 (Holocene) have been demarcated at depths 11.47 m, 4.68 m, 4.03 m, 18 m, and 21 m respectively in the core studied. MIS 5 section is characterized by alternating warm and cold periods as observed in Polar Ice cores. The main findings of this work indicates that the core site has recorded higher productivity with increased fluvial input during the warm, humid interglacial periods and interstadials than the stadials during the glacial period. However, the temporal variability from 150 kyr to 130 kyr has been considered as the glacial period with cold and dry climate that corresponding to the MIS 6, MIS 4 within this an episode of extremely low terrigenous input with heavier $\delta^{18}O$ values is noticed from 12.91 to 12.67 m. Similarly, a period of heavy $\delta^{18}O$ values, with less surface runoff and with low $\delta^{13}C$ values between 4.03 to 4.68 m bsf has been interpreted as MIS 4. Episodic fluctuation in SW monsoon induced productivity during MIS 3 has been observed in present study. The de-glacial event in MIS 2 marked in present core characterized by an abrupt increase in productivity during the mid-MIS 2.*

Keywords: *$\delta^{18}O$ and $\delta^{13}C$, Paleoclimate, paleomonsoon, piston core, south-eastern Arabian Sea.*

R*eceived 06 Nov., 2024;* ***R****evised 16 Nov., 2024;* ***A****ccepted 18 Nov., 2024 © The author(s) 2024.*
P*ublished with open access at* ***www.questjournas.org***

I. INTRODUCTION

The palaeoceanographic and palaeoclimatic reconstructions from the western and northern Arabian Sea, using planktic foraminiferal assemblages and geochemical proxies, have yielded profound insights into the variability of the South Asian/Indian monsoon over both short-term and long-time frames [1-11]. However, long-term information on late Quaternary fluctuations is needed which is crucial for evaluating the changes happened in different Glacial and inter-Glacial periods [12].

Sediments from the Arabian Sea serve as a valuable archive for paleoclimatic research. There are two monsoon systems in effect there: the Northeast (NE) monsoon (November to February) and the Southwest (SW) monsoon (June to September). The surface SW winds during the SW monsoon are landward and produce a lot

of precipitation. The winds that dominate the northeastern monsoon bring frigid, winter-like conditions to the Indian subcontinent. Recent data about past climate change from the Arabian Sea and Indian subcontinent indicate the varied nature of monsoon fluctuations.

Thamban and Purnachandra Rao [12] reconstructed alterations in regional hydrography linked to Indian monsoon variations during the late Quaternary. This reconstruction was based on the stable isotopic composition of foraminifera and organic matter found in three sediment cores extracted from the upper continental slope of western India. Somayajulu et al. [13] reconstructed redox conditions that existed in the northeastern continental margins of the Arabian Sea and the adjacent deep-water regions over the past few centuries. This was achieved using short, undisturbed sediment cores. The oxygen isotopic composition of individual specimens of surface-dwelling *Globigerinoides ruber* and *Globigerina bulloides*, extracted from sediment cores located in the Western Arabian Sea off Somalia, was employed to interpret past seasonal variations [14]. Researchers conducted multiple studies focusing on geochemical and paleontological aspects using sediment cores collected from various regions of the Arabian Sea.

The $\delta^{18}O$ composition of marine calcareous shells is primarily influenced by the temperature of shell calcification, local salinity variations, and variations in seawater composition. Surface salinity variations in tropical oceans are closely linked to the evaporation–precipitation (E–P) balance, serving as a significant climate indicator. The south-western continental margin of India currently exhibits relatively low salinity in comparison to other regions of the Arabian Sea, deviating from the typical latitudinal salinity patterns. The primary reason for this phenomenon is the significant influx of freshwater from the hinterland during the summer monsoon, coupled with the transport of low-salinity waters from the Bay of Bengal during the winter monsoon. Consequently, the planktic $\delta^{18}O$ composition in this region may have fluctuated historically due to local precipitation [12]. The present work illustrates the oxygen and carbon isotope records from a 13.4 m piston core in the southeastern Arabian Sea and examines their regional climate implications.

II. GEOLOGICAL SETTING

The study area is located in the mainland slope region between Lakshadweep Island and the southwestern part of the west coast of India (Fig 1).

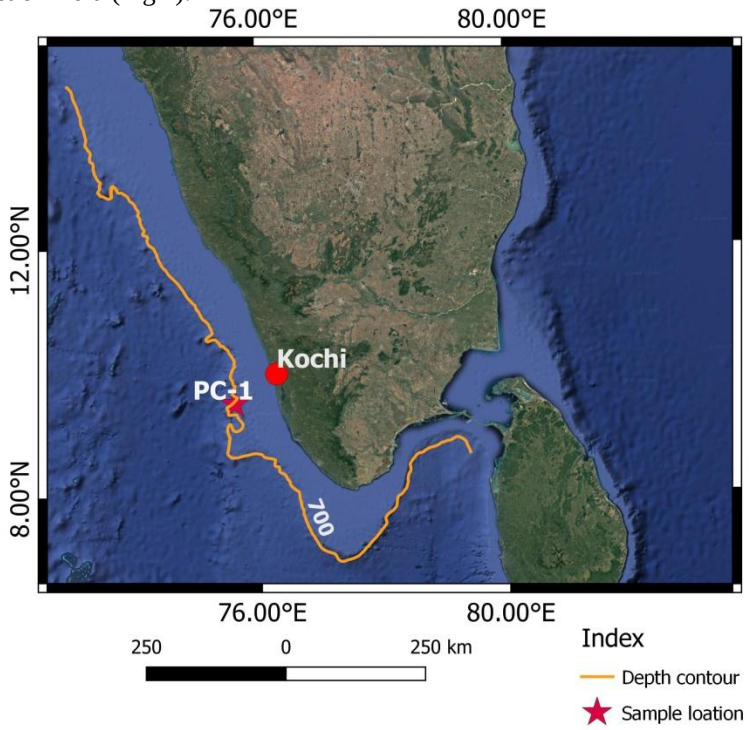

Figure1: Location of the core SR-004/PC-001, off Kochi.

This region experiences a tropical climate with an annual rainfall of approximately 1500 mm. The width of continental shelf in this area ranges from 70 to 78 km, while water depths vary from 1650 m in the northwest to 95 m in the east. The general slope is towards the west. The eastern part of the area is characterized by shallower, gentle, and relatively featureless terrain, with water depths ranging from 100 to 360 m. In contrast, the western part is steeper, with water depths ranging from 360 to 1650 m (Fig. 2). The

southwestern portion is shallower (500-800 m) and exhibits a distinctive channel feature with a width of 1-3 km and depths ranging from 110-250 m. A topographic high, varying in depth from 95 to 150 m, is present in the northern half of this area shown in Fig. 2. Additionally, a circular depression with a diameter of 600 m and a depth of 40 m is visible in the middle portion of the eastern area [15]. The shelf edge is straight and sharp, trending north-south in the northern part of the area (Fig. 2). However, in the southern part, the shelf edge is less defined, and its trend appears to be northeast-southwest due to shelf offsetting caused by down faulting. Bathymetric contours are closely spaced in the central area, indicating a steep slope, whereas they are widely spaced in the northern and southern regions, indicating gentler slopes. Steep gullies are observed on scarp faces in the northwestern and central parts due to sediment slumping from the slope (Fig 2).

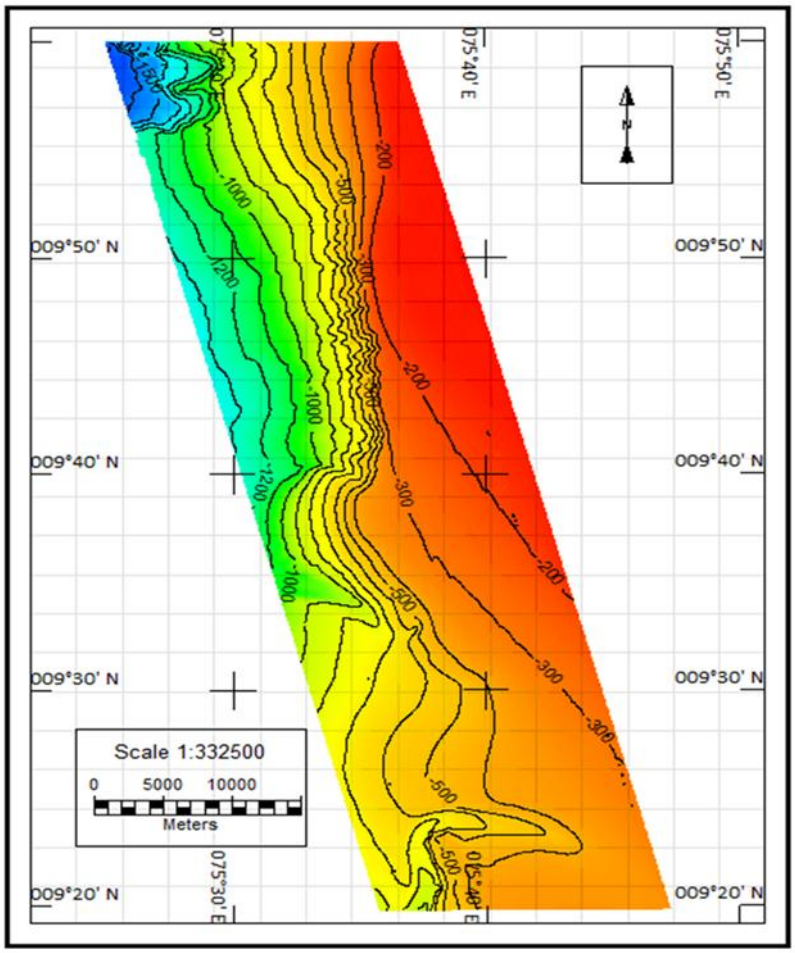

Figure2: Colored bathymetric map of the area, off Kochi.

The Periyar, Muvaatuupuzha, and Meenachil Rivers are the primary contributors of terrestrial sediments within the surveyed region. The Periyar River, Kerala's longest river, originates from the Sivagiri peaks (1,800 m) of Sundaramala in Tamil Nadu. Its course traverses a drainage basin characterized by pre-Cambrian crystalline formations, including charnockites, hornblende gneiss, garnet biotite gneiss, and minor biotite gneiss. Muvattupuzha River originates from the Western Ghats, draining through a highly diverse basin composed of pre-Cambrian crystalline formations, laterites, and Tertiary sedimentary rocks. Here, charnockites, hornblende-biotite gneisses, and other unclassified gneisses constitute a significant portion of the basin [16]. Meenachil River, a crucial waterway in Kottayam district, Kerala, begins its journey in the Western Ghats, coursing through the taluks of Meenachil, Vaikom, and Kottayam. The Meenachil river basin predominantly comprises pre-Cambrian metamorphic rocks, creating a hilly backdrop. Quartzite, charnokite, garnetiferous biotite gneiss, and pink/gray granite are among the major rock types found in the drainage basin [17].

III. MATERIALS AND METHODS

A sediment core, designated as PC-01 and spanning a length of 28 m, was collected from the south-eastern Arabian Sea during the R V Samudra Ratnakar (SR-004) cruise conducted by the Geological Survey of India. The top 13.7 m of the sediment core was studied as part of the Field Season Programs of RP-115 and RP-135 conducted by the Marine and Coastal Survey Division of the Geological Survey of India during 2017-18 and 2019-21.

The core was subsampled at intervals of 1 cm throughout its length. For every meter of the core, 25 samples were selected at 4 cm intervals for sedimentological and geochemical analysis. The samples for oxygen and carbon isotope studies were selected after studying the variation in the sedimentological and geochemical data. The sample thickness was kept to 1 cm to ensure a precise correlation of sedimentation with climatic events.

The individual splits of each sample were subjected to oven-drying at 60°C, followed by weighing and washing through a 63-µm stainless-steel mesh sieve. The resulting coarse sediment fraction (>63 µm) underwent dry sieving using 250- and 355-µm mesh sieves. Planktonic foraminiferal species, specifically *Globigerinoides ruber* (d'Orbigny, 1839), were manually selected from the 250- to 355-µm sediment fraction under a binocular microscope. These foraminiferal tests were immersed in methyl alcohol for several minutes and subsequently cleaned in an ultrasonic bath to eliminate adherent contaminants. After ultrasonic cleaning, excess methyl alcohol was removed using tissue paper, and any remaining alcohol was allowed to evaporate.

The foraminiferal samples were collected about <0.1 mg and composed of 10–20 specimens. The $\delta^{18}O$ and $\delta^{13}C$ of the shell samples were measured at high-resolution using a Thermo Finnigan MAT 253 isotope ratio mass spectrometer (IRMS) coupled with a Gas bench II in continuous flow mode stationed at Stable Isotope Laboratory, Centre for Earth Sciences, Indian Institute of Science, Bangalore and BSIP, Lukhnow. About 100 µg of carbonate powder was reacted with 1 ml of H_3PO_4 using the boat method [18] and the overall $\delta^{18}O$ reproducibility was ±0.08‰. All the carbon and oxygen isotopic values are reported on the VPDB scale using the internal lab standard of MAR-J1 as the primary standard.

IV. RESULTS AND DISCUSSION

Over the course of 2.5 million years of earth history, spanning the Quaternary period, the earth climate system has undergone numerous oscillations between glacial and interglacial states [19]. In the realm of paleooceanography, dating methodologies for Quaternary marine sediments have become increasingly vital for reconstructing paleoenvironments and paleoclimate. This study employed both relative and absolute dating methods to establish the chronology of events. It has been proposed that the incorporation of monsoon-associated freshwater, which contains lighter isotopes, is a primary factor affecting the oxygen isotope composition of the seawater in this area [19-21].

4.1 ABSOLUTE DATING

Radioisotope dating using ^{14}C is an absolute dating method. Three samples from different depths of the core, specifically from 0-1 cm, 99-100 cm, and 199-200 cm, underwent Accelerator Mass Spectrometry (AMS) ^{14}C dating at the Physical Research Laboratory in Ahmadabad [23]. The resulting ages were calculated as 5545 years, 31,433 years, and 42,569 years, respectively. The top 100 cm of the core corresponds to an age of 31,433 years, while the sediments at a depth of 200 cm yield an age of 42,569 years.

The age model of the core is constructed based on two calibrated AMS ^{14}C dated intervals, which are correlated with $\delta^{18}O$ records. Interestingly, the 0-1 cm interval also yielded an age of 5545 years. This discrepancy suggests the possibility of either sediment loss during core recovery or a lack of sedimentation in the area over the past 5545 years.

4.2 Relative dating

In this study, relative ages were determined by comparing stable isotope with the high-resolution data provided by Martison et al. (1984) [24]. The variation of $\delta^{18}O$ records down the core is depicted in Fig. 3.

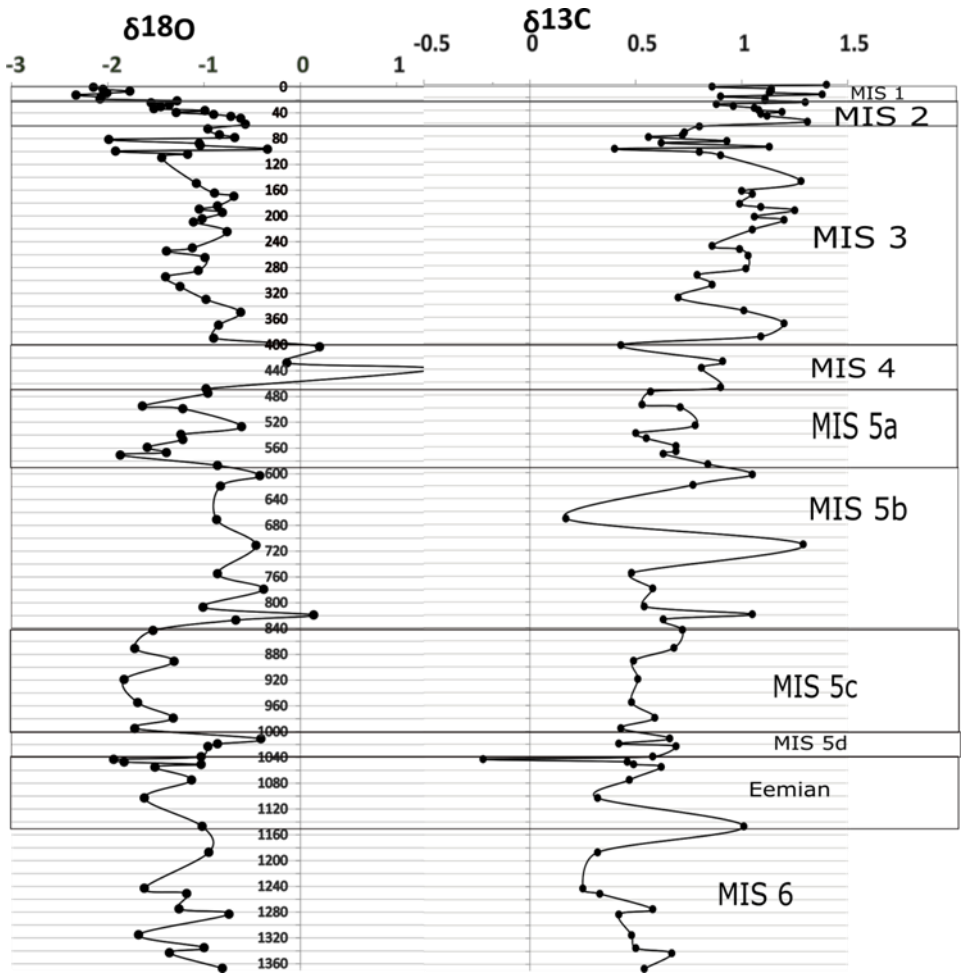

Figure 3: $\delta^{18}O$ and $\delta^{13}C$ of PC-001, off Kochin.

Additionally, a comparison between Martison's high-resolution data curves and the present data for each Marine Isotope Stage (MIS 1 to MIS 6) is presented in Fig. 4.

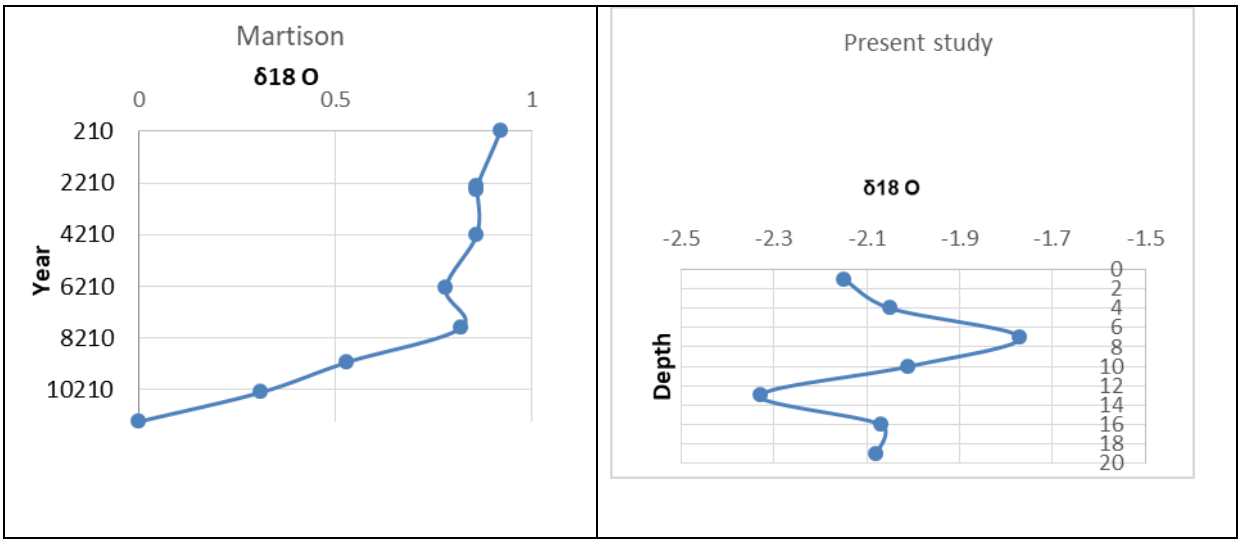

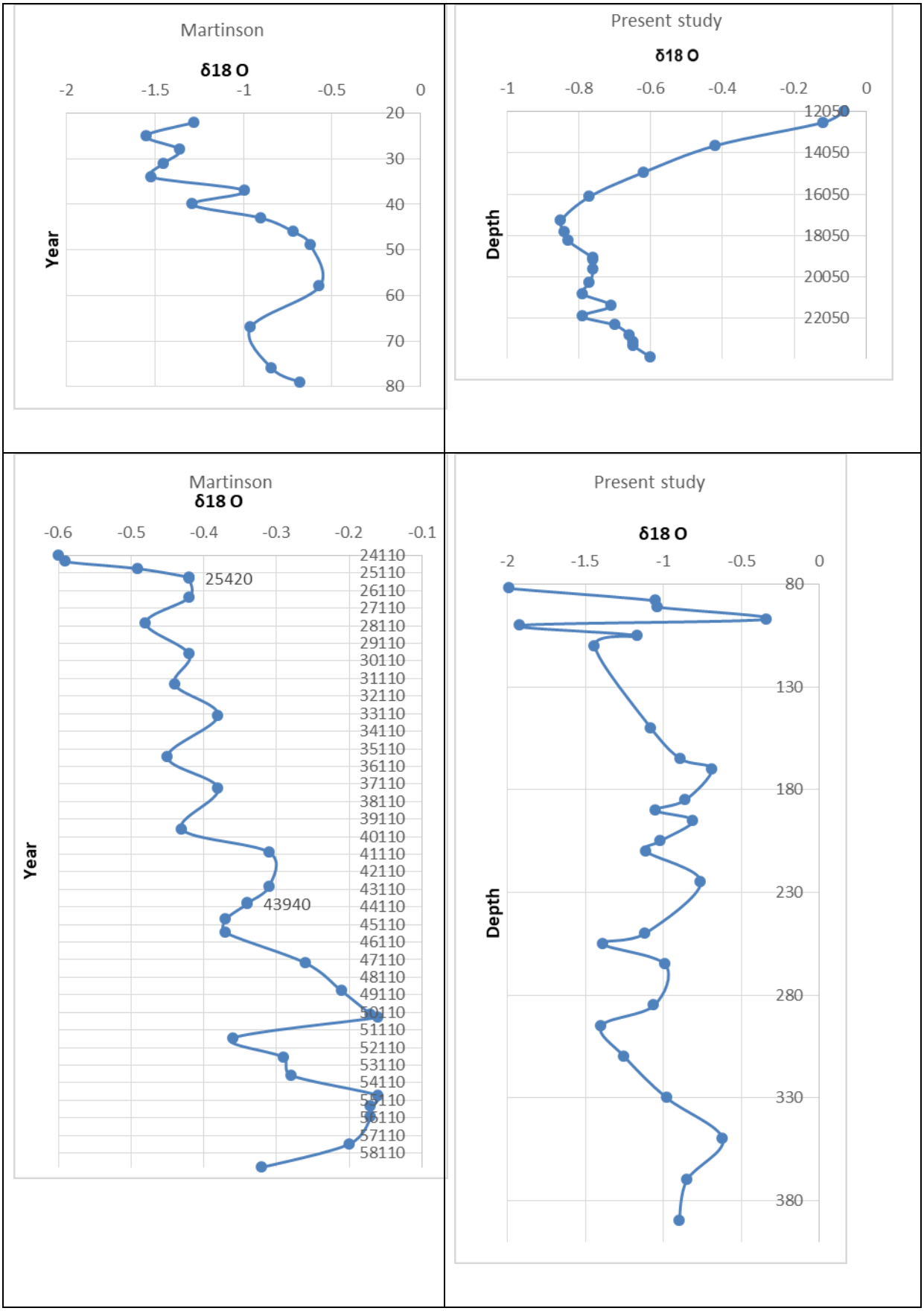
Martinson
δ18 O
-2
-1.5
-1
-0.5
0
Year
20
30
40
50
60
70
80
Present study
δ18 O
-1
-0.8
-0.6
-0.4
-0.2
0
Depth
12050
14050
16050
18050
20050
22050
Martinson
δ18 O
-0.6
-0.5
-0.4
-0.3
-0.2
-0.1
Year
25420
43940
Present study
δ18 O
-2
-1.5
-1
-0.5
0
Depth
80
130
180
230
280
330
380

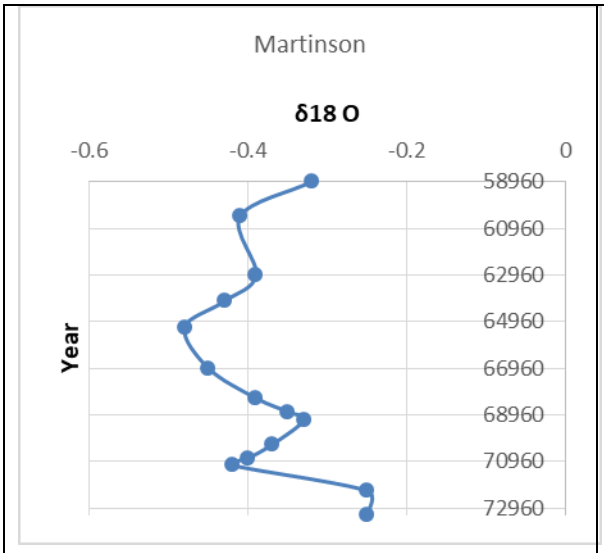
Martinson
δ18 O
-0.6
-0.4
-0.2
0
Year
58960
60960
62960
64960
66960
68960
70960
72960

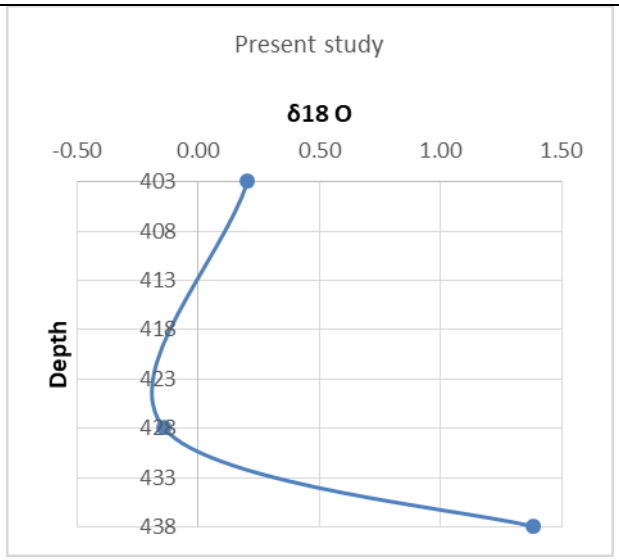
Present study
δ18 O
-0.50
0.00
0.50
1.00
1.50
Depth
403
408
413
418
423
428
433
438

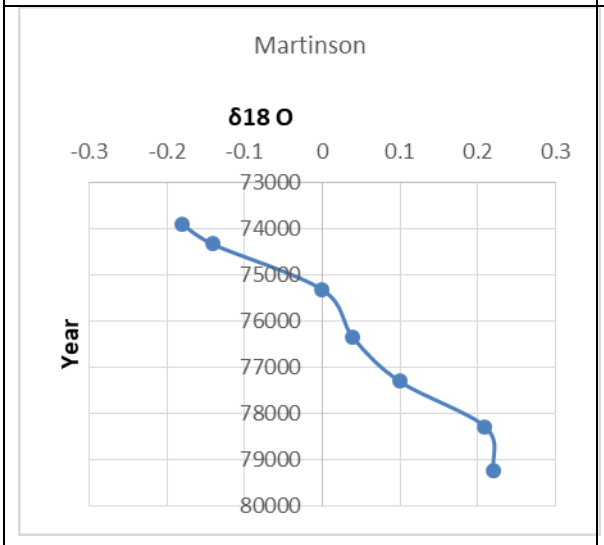
Martinson
δ18 O
-0.3
-0.2
-0.1
0
0.1
0.2
0.3
Year
73000
74000
75000
76000
77000
78000
79000
80000

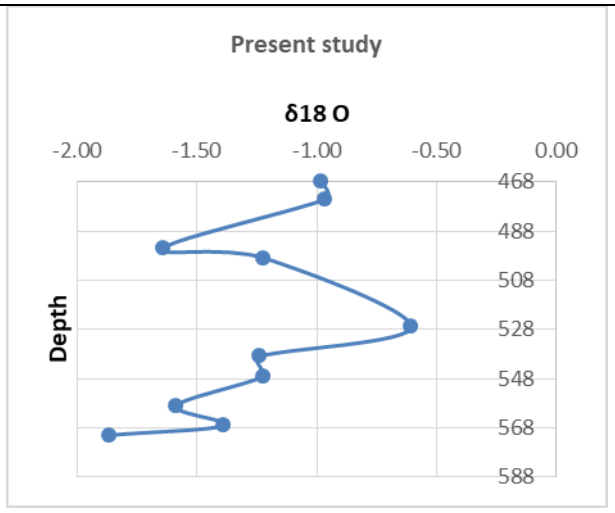
Present study
δ18 O
-2.00
-1.50
-1.00
-0.50
0.00
Depth
468
488
508
528
548
568
588

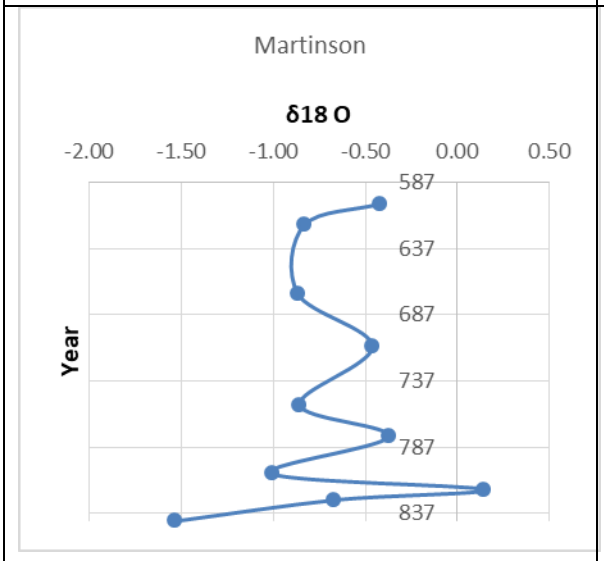
Martinson
δ18 O
-2.00
-1.50
-1.00
-0.50
0.00
0.50
Year
587
637
687
737
787
837

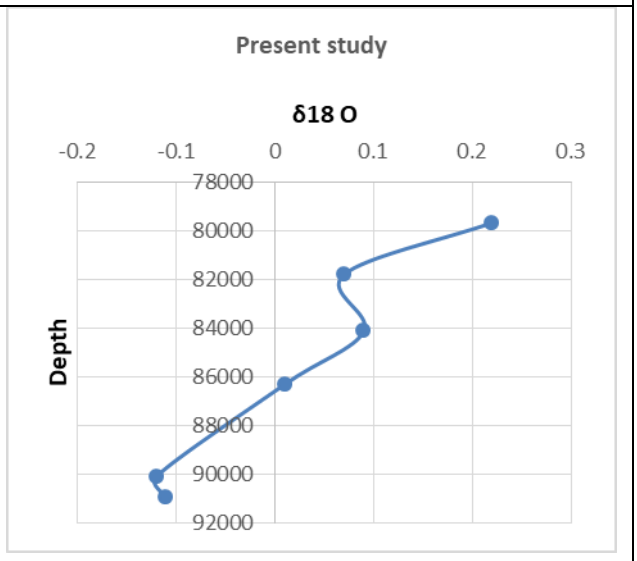
Present study
δ18 O
-0.2
-0.1
0
0.1
0.2
0.3
Depth
78000
80000
82000
84000
86000
88000
90000
92000

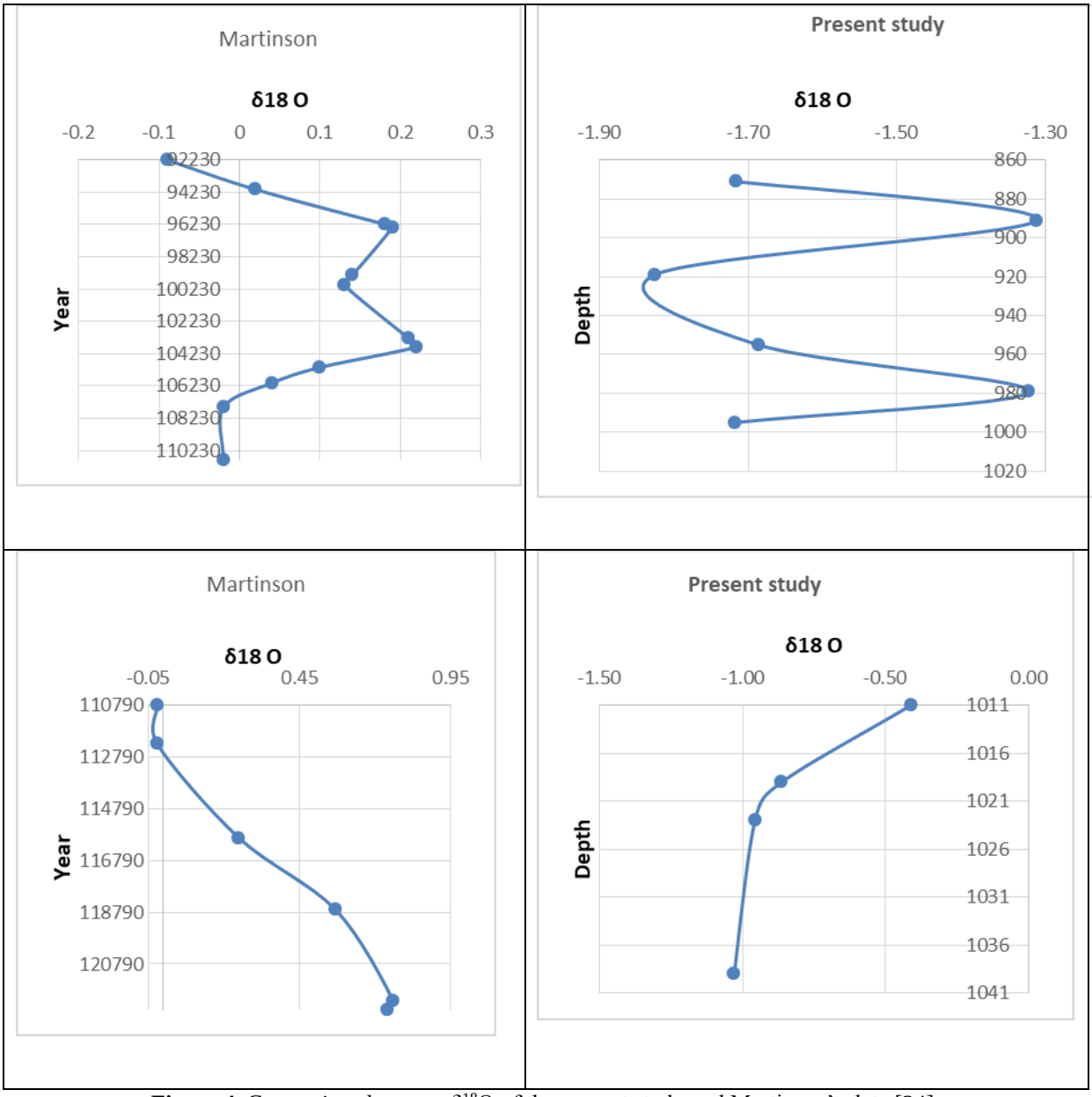

Figure 4. Comparison between $\delta^{18}O$ of the present study and Martinson's data [24].

These comparisons aid in establishing the relative chronology of events in the core sediment.

Oxygen isotope

The radiocarbon (^{14}C) method can determine ages up to approximately 55,000 years, which is about 10 half-lives of radioactive carbon. The AMS-based ^{14}C age of the core at 200 cm level showed an age of 42,569 yrs and thus the further downward portion of the core cannot be dated using the ^{14}C method Palaeogeography Palaeoclimatology Palaeoecology values are a good indicator of climatic events and can be used as a method for relative dating of these geological archives [25]. The $\delta^{18}O$ composition of surface-dwelling planktic foraminifera Globigerinoides ruber (400–450 micron size) has been utilized to reconstruct past surface water conditions. The evaporation and precipitation play significant roles in altering the ratio of heavy to light oxygen isotopes in the oceans. When water evaporates, the lighter isotope of oxygen, ^{16}O, evaporates more rapidly, leading to an enrichment of the oceans with the heavier ^{18}O. Subsequently, when these water vapors precipitate in polar regions, the ^{16}O gets trapped in polar ice, persisting throughout colder periods in earth history. During such periods, foraminifera shells from the oceans exhibit higher ^{18}O concentrations or more positive $\delta^{18}O$ values. Conversely, during warmer periods, $\delta^{18}O$ values become lighter or more negative due to the release of the lighter isotope previously trapped in polar regions during melting.

Additionally, $\delta^{18}O$ values are influenced by factors like salinity and temperature during shell calcification. The southwestern continental margin of India, for example, experiences unique conditions due to a substantial influx of freshwater during the summer monsoon and the transport of low-salinity water from the Bay of Bengal during the winter monsoon. As a result, this region exhibits lower salinity compared to other parts of the Arabian Sea and does not follow typical salinity variations based on latitudinal positions alone. Consequently, it is inferred that the planktic $\delta^{18}O$ composition in this area may have varied historically based on local precipitation patterns [12].

Marine Isotope Stages indicate alternating glacial-interglacial periods of earth history, inferred from oxygen isotope data. With the limited sampling resolution in the core, the $\delta^{18}O$ records exhibit distinct glacial-interglacial stages. The even-numbered MIS stages represent glacial periods with heavier $\delta^{18}O$ values, while odd-numbered stages represent interglacial periods with lighter $\delta^{18}O$ values. During Isotope Stage 5, all interstadials (5a, 5b, and Eemian) and stadials (5b and 5d) were identified based on the $\delta^{18}O$ record.

The stable oxygen isotope records of *Globigerinoides ruber* from 0 to 13.7 m in the studied core, displayed in Fig. 2, exhibit $\delta^{18}O$ values ranging from -1.94 to 1.39‰. These values are compared with adjacent core's oxygen isotope data and correlated with SPECMAP data and high-resolution data from [24], aiding in identifying MIS boundaries in the core. The boundary between MIS 1/MIS 2 at 0.21 m bsf and MIS 2/MIS 3 at 0.81 m bsf was established from the top 4 m of the core. The boundary between MIS 3 and MIS 4 is demarcated at 4.03 m depth due to data fluctuations of 1.13‰ $\delta^{18}O$ value. The highest $\delta^{18}O$ value is observed at 4.38 m bsf, characterizing MIS 4 stages in the area from 4.03 to 4.68 m bsf of the core. The MIS 4/MIS 5 boundary is identified around 4.68 m, where $\delta^{18}O$ varies from -0.98 to 1.39‰. Similarly, the MIS 5/MIS 6 boundary is set at 11.47 m bsf, where $\delta^{18}O$ fluctuates by about 0.6‰. However, the MIS 6/MIS 7 boundary remains untraceable within the top 13.7 m of the core.

Carbon isotope

In carbon isotope studies for paleoclimatic reconstruction, similar to oxygen isotope analysis, the values of two carbon isotopes, ^{12}C (lighter) and ^{13}C (heavier), are compared. These comparisons are made by measuring a sample with a mass spectrometer and then comparing its values to those of a known isotopic reference standard. Photosynthesis, respiration, and ocean water upwelling are the primary factors influencing the carbon isotopes found in planktic foraminifera shells. During geological periods with increased photosynthesis activity, photosynthesizing organisms absorb more ^{12}C, making more ^{13}C available in the water for foraminifera to use in building their shells. Higher productivity levels also lead to increased burial, resulting in a more positive $\delta^{13}C$ value, indicating greater productivity. Conversely, a rise in $\delta^{13}C$ values can suggest reduced erosion from the terrestrial realm.

Soil typically exhibits a more negative $\delta^{13}C$ value due to the presence of ^{12}C ions from decomposed plants. When this soil enters the ocean, it enriches the water with ^{12}C ions. In regions with upwelling, nutrient-rich older water, containing higher concentrations of ^{12}C, rises to the surface. Under these conditions, foraminifera shells exhibit a more negative $\delta^{13}C$ signal. The $\delta^{13}C$ values for Globigerinoids ruber ranging from -0.22 (10.43 mbsf, Eemian) to 1.29‰ (7.11 mbsf, MIS 5b). On average, these values show a $\delta^{13}C$ value of 0.59‰.

Based on the comparison of $\delta^{18}O$ values with the SPECMAP, the last identified stage within the top 13.7 m bsf of the core is MIS 6, spanning from 191 to 130 kilo years ago (kyr). The boundary between MIS 5 and MIS 6 is determined at 11.47 m bsf, marked by an increase in $\delta^{18}O$ values thereafter. MIS 6 is characterized as a glacial stage with heavier $\delta^{18}O$ values ranging from -1.68 to -0.74‰ and averaging at -1.16‰. However, the boundary between MIS 6 and MIS 7 could not be identified within the 13.7 m segment of the core. From 11.43 ms below seafloor (m bsf) and beyond, $\delta^{13}C$ values range from 0.32‰ at 12.51 m bsf to 0.67‰ at 13.43 m bsf, with an average of 0.51‰. These values are lower compared to those of Marine Isotope Stage 5 (MIS 5), indicating reduced productivity in the area during this glacial period. The heavier $\delta^{18}O$ ratio observed at this depth is characteristic of the glacial period, and the low $\delta^{13}C$ ratios further support this interpretation (Fig. 3).

The transition from MIS 4 to MIS 5, representing the last major interglacial episode in earth climate history, is delineated within the core from 4.68 to 11.47 m below seafloor (m bsf). The boundary between MIS 4 and MIS 5 is set at 4.68 m bsf, marked by a 2.37‰ decrease in $\delta^{18}O$ value. Within this segment, $\delta^{18}O$ values range from -1.94 to 0.14‰. MIS 5 is further subdivided into five sub-stages denoted as 5a to 5e, with peak stages identified at 82, 87, 96, 109, and 123 thousand years respectively [26]. The demarcation between MIS 5a and MIS 5b occurs at 5.87 m below the seafloor, characterized by a sudden increase of 1.01‰ in $\delta^{18}O$ value. The interval from 5.87 to 8.43 m bsf displays relatively higher isotope values, with an average of -0.62‰, suggesting a cold phase during MIS 5. A sudden increase in $\delta^{18}O$ value is observed at 8.43 m bsf, indicating the

transition between MIS 5b and MIS 5c. The demarcation between MIS 5b and MIS 5c is established at 8.43 m below sea floor, corresponding to lighter $\delta^{18}O$ values of approximately 0.87‰. In this range, $\delta^{18}O$ values vary from -1.83‰ to -1.31‰, with an average of -1.59‰, suggesting a warm period during MIS 5. The boundary between MIS 5c and MIS 5d is established at 10.11 m below sea floor, corresponding to elevated $\delta^{18}O$ values of approximately 1.31‰. This segment displays heavier isotope ratios averaging -0.82‰, suggesting a colder phase during MIS 5. The transition between MIS 5d and the Eemian period is characterized by a rapid decline in $\delta^{18}O$ value of about 0.60‰ at a depth of 11.47 m below the surface. The Eemian period, the most recent interglacial prior to the current one, extends from 10.43 to 11.47 meters below the seafloor in the core. Notable $\delta^{18}O$ values span from -0.95‰ to -1.94‰, with the latter representing the lightest value within the 4 to 13.7 m bsf range, in proximity to the $\delta^{18}O$ value at the MIS 3/MIS 2 boundary. The lower $\delta^{18}O$ values suggest a warmer climate during MIS 5, analogous to current climate projections. The Eemian period offers insights into sea-level fluctuations, characterized by levels several meters higher than those of today and significant variations throughout the period. The shift from MIS 5d to the Eemian is characterized by a rapid decline in $\delta^{18}O$ value of approximately 1.31‰ at a depth of around 10.11 m below the surface. The importance of climatic changes during the Eemian period is evident in its similarity to the expected climatic alterations of the present day. Sources indicate that during the Eemian, as per Marine Isotope Stage 5, temperatures were approximately 2 degrees Celsius higher than pre-industrial levels, and potentially 1 degree Celsius above current levels. The peak temperatures of the Eemian were only slightly higher than present-day temperatures, as observed by Bazin et al. in [27].

Understanding the Eemian era offers insights into potential sea-level variations under sustained global temperature increases. Records indicate that Eemian sea levels rose several meters above today's levels, as supported by studies from [28-33]. During the Eemian, sea levels fluctuated by approximately 1 meter per century, according to research by Rohling et al. [34], Thompson et al. [35], and Blanchon et al. [36].

In Marine Isotope Stage 5 (MIS 5), $\delta^{13}C$ values range from -0.22‰ at 10.75 meters below seafloor (m bsf) (Eemian) to 1.29‰ at 7.11 m bsf (MIS 5c) within the core's depth of 4.68 to 11.43 m bsf. The average $\delta^{13}C$ value for this period is 0.62‰. MIS 5 is characterized by warm periods interspersed with cold periods, represented by five sub-stages. During the warm periods, such as MIS 5a and MIS 5c, $\delta^{13}C$ values are more positive, indicating higher productivity compared to the colder period, MIS 5d. The lowest $\delta^{13}C$ value at 10.75 m bsf during the Eemian may be attributed to increased runoff from the land, suggesting a high intensity of summer monsoon during this time. Similarly, the high $\delta^{13}C$ value at 8.19 m bsf in the colder period of MIS 5b may result from decreased runoff from the land rather than reduced productivity.

The transition from MIS 3 to MIS 4 is notable for a significant shift from lower (-0.9) to higher (0.2) $\delta^{18}O$ values, indicating an increase in the evaporation-precipitation budget in the East Asian Seas (EAS), possibly due to a weakening of the southwest (SW) monsoon. The MIS 4 event in the core is identified from 4.03 to 4.68 meters below seafloor (m bsf), with $\delta^{18}O$ values ranging from -0.98 to 1.39‰ and averaging at 0.12‰. The highest $\delta^{18}O$ value of 1.39‰ occurs at a depth of 4.38 m bsf within MIS 4. Despite the low sample density in this 65 cm section of the core, the heavier average $\delta^{18}O$ value supports its classification as the MIS 4 stage. Comparatively, MIS 4 exhibits higher $\delta^{18}O$ values than MIS 2. In MIS 2, at 0.58 m bsf, the $\delta^{18}O$ value shifted to heavier levels but subsequently decreased. Hence, the depth of 0.58 m can be considered the glacial maximum, after which a deglaciation event likely commenced. Similarly, in MIS 4, at 4.38 m where the highest $\delta^{18}O$ value is recorded, may represent the glacial maximum within that stage.

In the segment from 4.03 to 4.68 meters below seafloor (m bsf) of the core, the $\delta^{13}C$ values exhibit a decrease, ranging from 0.33‰ at 4.68 m to 0.25‰ at 4.38 m, with an average of 0.25‰. The lower $\delta^{13}C$ values during this period signify reduced productivity in the area. These low $\delta^{13}C$ values, combined with the heavier $\delta^{18}O$ values, align with categorizing this period as the MIS 4 glaciation phase.

The $\delta^{18}O$ values during MIS 3 range from -1.99 to -0.34‰, with an average of -1.06‰. The boundary between MIS 2 and MIS 3 is established at 0.81 meters due to significant fluctuations in $\delta^{18}O$ values, amounting to approximately 1.3‰. Globally, the period of 24 to 60 thousand years ago within MIS 3 witnessed numerous abrupt climatic warming phases known as Dansgaard–Oeschger (DO) events. These events are identifiable in Greenland ice core oxygen isotope records, characterized by swift transitions from cold, stadial climates to mild, interstadial conditions, followed by a return to cold stadial conditions [37]. Additionally, certain stadials within this period saw massive ice surges from the Laurentide Ice Sheet, leading to Heinrich events [38], where substantial ice was discharged into the North Atlantic Ocean.

The frequency of DO events during MIS 3 contrasts with their rarity around the Last Glacial Maximum (LGM), a phenomenon not yet fully understood. In the studied core, spanning 3.08 meters (from 0.81 to 3.95 meters), which corresponds to MIS 3, stadials and interstadials are evident. Monsoon reconstructions based on

$\delta^{18}O$ indicate higher monsoon-driven precipitation during MIS 1 and MIS 3, contrasting with lower precipitation during MIS 2. This aligns with earlier monsoon reconstructions derived from upwelling indices in the western Arabian Sea. Studies conducted by Owen et al. [39] indicate that Marine Isotope Stage 3 (MIS 3) was characterized by elevated insolation, coinciding with a strengthening of the South Asian Monsoon following Marine Isotope Stage 4 (MIS 4). The present study reveals elevated $\delta^{18}O$ values at the core's base, indicative of late MIS 3. A gradual decline in $\delta^{18}O$ occurs during the transition from MIS 3 to MIS 2, implying a warmer climate accompanied by increased precipitation. This may have facilitated the intrusion of low salinity Bay of Bengal water into the core site, leading to an increase in ^{16}O isotopes and a depletion of ^{18}O isotopes, ultimately resulting in a decrease in $\delta^{18}O$ values within the sediments [23].

Between depths of 0.81 to 4.03 meters below seafloor (m bsf) of the core, the $\delta^{13}C$ values range from 0.4‰ at 99.5 m bsf to 1.28‰ at 149.5 m bsf, with an average of 0.95‰. A higher $\delta^{13}C$ value indicates increased productivity in the area. This observation is consistent with the lighter $\delta^{18}O$ values obtained from this core segment, which helped identify this period as the MIS 3 interglacial. Although variations between stadials and interstadials were noticeable, pinpointing their exact boundaries was challenging due to the limited data density in this stage.

The MIS 2/MIS 3 boundary is pinpointed at 81.5 cm below seafloor (bsf), marked by a significant fluctuation of $\delta^{18}O$ values around 1.3‰. Core depth 21-81.5 cm representing MIS 2/LGM to De-Glacial phase marked by a significant fluctuation of $\delta^{18}O$ values around 1.3‰. a phase of heaviest $\delta^{18}O$ values is observed between 80 and 60 cm bsf, signifying the Last Glacial Maximum (LGM) events. A gradual decrease in $\delta^{18}O$ values between 60 and 21 cm bsf indicates the De-glacial event, with lower $\delta^{18}O$ values suggesting increased freshwater run-off from the hinterland induced by the strengthened Southwest (SW) monsoon. Another oscillation in $\delta^{18}O$ values is noted at approximately 20 cm bsf, with fluctuations of about 0.8‰, marking the MIS 1/MIS 2 boundary. The top 20 cm of the core representing the MIS 1/Holocene phase.

V. Conclusions

This study reveals distinct boundaries corresponding to glacial-interglacial cycles over the spans approximately 150 thousand years from the present. The last identified stage in the core is Marine Isotope Stage 6 (MIS 6), covering the period from 150 to 130 thousand years before present (kyr) which represent 11.47 m. The MIS 6/MIS 5 boundary is determined at 11.47 m bsf based on the variation in $\delta^{18}O$ values. Within the core, five sub-stages of MIS are identified from 10.47 to 4.68 m bsf. The peak of the Eemian period (MIS 5e) to MIS 5a is fixed at depths of 10.43, 10.11, 8.43, and 5.87 meters, respectively. These stages are characterized by alternating heavier and lighter $\delta^{18}O$ values, indicating glacial and interglacial events. Stadials such as MIS 5b and MIS 5d exhibit heavier $\delta^{18}O$ values, signaling colder climates in the region. Conversely, interstadials including MIS 5a, MIS 5c, and the Eemian are marked by lighter $\delta^{18}O$ values, indicating warmer climates at the core site. Several studies have established a more intense monsoon in the western continental margin of India during the Pleistocene-Holocene transition, based on palaeo-climatic proxy records in sediment cores [40-43].

REFERENCES

[1]. Clemens, S., W. L. Prell, D. Murray, G. B. Shimmield, and G. Weedon, Forcing mechanisms of the Indian Ocean monsoon. Nature, 1991. **353:** p 720–725.

[2]. Anderson, D. and W. Prell, A 300 kyr record of upwelling off Oman during the Late Quaternary: evidence of the Asian southwest monsoon. Paleoceanography, 1995. **8:** p 193–208.

[3]. Vénec-Peyré, M., J. Caulet and C. Grazzini, Paleohydrographic changes in the Somali Basin (5°N upwelling and equatorial areas) during the last 160 kyr, based on correspondence analysis of foraminiferal and radiolarian assemblages. Paleoceanography, 1995. **10:** p 473–491.

[4]. Naidu, P. and B. Malmgren, A high-resolution record of Late Quaternary upwelling along the Oman Margin, Arabian Sea based on planktonic foraminifera. Paleoceanography, 1996. **11:** p 129–124.

[5]. Reichart, G., L. Lourens and W. Zachariasse, Temporal variability in the northern Arabian Sea oxygen minimum zone (OMZ) during the last 225,000 years. Paleoceanography, 1998. **13:** p 607–621.

[6]. Schulz, H., U. Von Rad and H. Erlkeuser, Correlation between Arabian Sea and Greenland climate oscillations of the past 110,000 years. Nature, 1998. **393:** p 54–57.

[7]. Schulte, S. and P. Müller, Variations of sea surface temperature and primary productivity during Heinrich and Dansgaard-Oeschger events in the northeastern Arabian Sea. Geo-Marine Letters, 2001. **21:** p 168–175.

[8]. Jung, S., E. Ivanova, G. Reichar, G. Davies, G. Ganssen, D. Kroon and J. Van Hinte, Centennial-millennial-scale monsoon variations off Somalia over the last 35 ka. In: The Tectonic and Climatic Evolution of the Arabian Sea Region (eds P.D. Clift, D. Kroon, C. Gaedicke and J. Craig), Special Publication no. 195, 2002 p. 341–52. Geological Society of London.

[9]. Gupta, A., D. Anderson and J. Overpeck, Abrupt changes in the Asian southwest monsoon during the Holocene and their links to the North Atlantic Ocean. Nature, 2003. **421**: p 354–357.

[10]. Ivanova, E., R. Schiebel, A.D.Singh, G. Schmiedl, H. Niebler and C. Hemleben, Primary production in the Arabian Sea during the last 135 000 years. Palaeogeography Palaeoclimatology Palaeoecology,2003. **197**: p 61–82.

[11]. Ivanochko, T., R. Ganeshram, G. Brummer, G. Ganssen, S. Jung, S. Moreton and D. Kroon, Variations in tropical convection as an amplifier of global climate change at the millennial scale, Earth Planetary Sciences Letters 2005. **235:** p 302–314.

[12]. Thamban, M., V. Purnachandra Rao, New stable isotope records of sediment cores from the SE Arabian Sea – Inferences on the variations in monsoon regime during the late Quaternary, Current Science, 2011. **80**(11).

[13]. Somayajulu, B.L.K., D.N. Yadav and M.M. Sarin, Recent sedimentary records from the Arabian Sea. Proceedings of the Indian Academy of Sciences - Earth Planetary Sciences, 1994. **103**(2): p 315-327.

[14]. Ganssen, GM., F.J.C. Peeters, B. Metcalfe, P. Anand, S.J.A. Jung, D. Kroon, G.-J.A. Brummer, Quantifying sea surface temperature ranges of the Arabian Sea for the past 20 000 years. Climate of the Past, 2011. **7:** p 1337–1349.

[15]. Pillai et al., 2016, Geological Survey of India Report, Unpublished.

[16]. Maya, K., Studies on the nature and chemistry of sediments and water of Periyar and Chalakudy rivers, Kerala, India. Ph.D. Thesis (Unpublished), (2005) Cochin University of Science and Technology, Kochi, India.

[17]. Padmalal, D. Mineralogy and Geochemistry of the sediments of Muvattupuzha river and Central Vembanad estuary, Kerala, India, Ph.D. Thesis, 1992, (Unpublished). (1992) Cochin University of Science and Technology, Kochi, India.

[18]. Rangarajan, R., High Resolution Reconstruction of Rainfall Using Stable Isotopes in Growth Bands of Terrestrial Gastropod. Ph.D. Thesis, 2014, Indian Institute of Science.

[19]. Walker, M. Quaternary Dating Methods, 2005, New York, NY: John Wiley and Sons.

[20]. Duplessy, J.-C., Nature, 1982. **295:** p 494–498.

[21]. M. Thamban, V.P. Rao, R.R. Schneider and P.M. Grootes, Palaeogeography Palaeoclimatology Palaeoecology, 2001. **165:** p 113–127.

[22]. Ashish-Sarkar, R. Ramesh, B.L.K. Somayajulu, R. Agnihotri, A.J.T. Jull and G.S. Burr, Earth Planetry Science Letters, 2000. **177:** p 209–218.

[23]. Shaniba, V. et al., Variation of Late Quaternary productivity and associated monsoonal intensity in the southwestern continental margin of India, Indian Journal of Geosciences, 2024. **76**(4).

[24]. Martinson, D.M. , N.G. Pisias, J.D. Hays, J. Imbrie, T.C. Moor Jr, N.J. Shackleton, "Age dating and the orbital theory of the ice ages: development of a high resolution 0 to 300000 year chronostratigraphy" Quaternary Research, 1987. **27:** p 1-29.

[25]. Pisias, N.G, D.G. Martinson, T.C. Moore, N.J. Shackleton, W.L. Prell, J.D. Hays, G. Boden, High resolution stratigraphic correlation of benthic oxygen isotope records spanning the last 300,000 years, Marine Geology, 1984. **56:** p 119–136.

[26]. Shackleton, N.J., The last interglacial in the marine and terrestrial record. Proceedings of the Royal Society London, B, 1969. **174:** p 135–154.

[27]. Bazin, L., A. Landais, B. Lemieux-Dudon, H. Toye Mahamadou Kele, D. Veres, F. Parrenin, P. Martinerie, C. Ritz, E. Capron, V. Lipenkov, M.F. Loutre, D. Raynaud, B. Vinther, A. Svensson, S.O. Rasmussen, M. Severi, T. Blunier, M. Leuenberger, H. Fischer, V. Masson-Delmotte, J. Chappellaz and E. Wolff, An optimized multi-proxy, multi-site Antarctic ice and gas orbital chronology (AICC2012): 120-800 ka, Climate of the Past, 2013. **9:** p 1715-1731.

[28]. Chen, J.H., H.A. Curran, B. White, G.J. Wasserburg, Precise chronology of the last interglacial period: 234U-230 25 Th data from fossil coral reefs in the Bahamas, Geological Society of America Bulletin, 1991. **103:** p 82–97.

[29]. Neumann, A.C., P.J. Hearty, Rapid sea-level changes at the close of the last interglacial (substage 5e) recorded in Bahamian island geology, Geology, 1996. **24:** p775–778.

[30]. Hearty, P.J., J.T. Hollin, A.C. Neumann, M.J. O'Leary, M. McCulloch, Global sea-level fluctuations during the Last Interglaciation (MIS 5e)," Quaternary Science Review, 2007. **26:** p 2090–2112.

[31]. Kopp, R.E., F.J. Simons, J.X. Mitrovica, A.C. Maloof, M. Oppenheimer, Probabilistic assessment of sea level during the last interglacial stage, Nature, 2009. **462:** p 863–867.

[32]. Dutton, A., K. Lambeck, Ice volume and sea level during the last interglacial, Science, 2012. **337:** p 20216–20219.

[33]. O'Leary, M.J., P.J. Hearty, W.G. Thompson, M.E. Raymo, J.X. Mitrovica, J.M. Webster, Ice sheet collapse following a prolonged period of stable sea level during the last interglacial, Nature Geoscience, 2013 **6:** p 796–800.

[34]. Rohling, E.J., K. Grant, Ch. Hemleben, M. Siddall, B.A.A. Hoogakker, M. Bolshaw, M. Kucera, "High rates of sea-level rise during the last interglacial period," Nature Geoscience, 2008. **1:** p 38–42.

[35]. Thompson, D.W.J., S. Solomon, P.J. Kushner, M.H. England, K.M. Grise, D.J. Karoly, Signatures of the Antarctic ozone hole in Southern Hemisphere surface climate change, Nature Geoscience, 2011. **4:** p741–749.

[36]. Blanchon, P., A. Eisenhauer, J. Fietzke, V. Liebetrau, "Rapid sea-level rise and reef backstepping at the close of the last interglacial highstand, Nature, 2009. **458:** p 881–885.

[37]. Dansgaard , W., S.J. Johnsen, H.B. Clausen, D. Dahl-Jensen, N.S. Gundestrup, C.U. Hammer, C.S. Hvidberg, J.P. Steffensen, A.E. Sveinbjornsdottir, J. Jouzel and G. Bond, Evidence for general instability of past climate from a 250-kyr ice-core record. Nature, 1993. **364:** p 218–220.

[38]. Heinrich, H., Origin and consequences of cyclic ice rafting in the Northeast Atlantic Ocean during the past 130,000 years. Quaternary Research, 1998. **29:** p 142–152.

[39]. Owen, L.A., R.C. Finkel and M.W. Caffee, A note on the extent of glaciation throughout the Himalaya during the global Last Glacial Maximum. Quaternary Science Review, 2002. **21:** pp 147–157.

[40]. Van Campo, E., Monsoon fluctuations in two 20,000 yrs BP oxygen isotope /pollen records of southwest India. Quaternary Research, 1986. **26:** p 376– 388.
[41]. Prell, W.L., R.E. Marvil and M.E. Luther, Variability in upwelling fields in the northwestern Indian Ocean 2. Data-model comparison at 9000 years B.P. Paleooceanography, 1990. **5:** p 447-457.
[42]. Naidu P.D., and B.A. Malmgren, A high-resolution record of late Quaternary upwelling along the Oman Margin, Arabian Sea based on planktonic foraminifera. Paleoecology, 1996. **11**: p 129-140.
[43]. Rajagopalan, G., R. Sukumar, R. Ramesh, R.K. Pant, Late Quatemary vegetational and climatic changes from tropical peats in southern India—An extended record up to 40,000 years B. Current Science, 1997. **73**(1): p 60-63.